Simple Energy-Based Method for Estimating the Equivalent Circuit Parameters of Electrolytic Capacitors

Published Version:
Sandrolini, L., Simonazzi, M., Mariscotti, A., Pasini, G. (2023). Simple Energy-Based Method for Estimating the Equivalent Circuit Parameters of Electrolytic Capacitors. Piscatawey (NJ) : IEEE [10.1109/emceurope57790.2023.10274166].

Availability:
This version is available at: https://hdl.handle.net/11585/963004 since: 2025-01-24

Published:
DOI: http://doi.org/10.1109/emceurope57790.2023.10274166

Simple Energy-Based Method for Estimating the Equivalent Circuit Parameters of Electrolytic Capacitors

Leonardo Sandrolini
DEI
University of Bologna
Bologna, Italy
leonardo.sandrolini@unibo.it

Mattia Simonazzi
DEI
University of Bologna
Bologna, Italy
mattia.simonazzi2@unibo.it

Andrea Mariscotti
DITEN
University of Genova
Genova, Italy
andrea.mariscotti@unige.it

Gaetano Pasini
DEI
University of Bologna
Bologna, Italy
gaetano.pasini@unibo.it

***Abstract*—A simple method based on the energy conservation principle is proposed for the estimation of the equivalent circuit parameters of electrolytic capacitors. A series R-L-C circuit model is chosen to describe the real behaviour of these components, which are increasingly used in power converters to realize the DC-bus and filter the generated electromagnetic interference (EMI). The proposed method allows electrolytic capacitors to be characterised in any operating condition and requires only the measurement of the voltage and current waveforms of the capacitor under test.**

***Index Terms*—Electromagnetic compatibility, electrolytic capacitors, ESR, ESL, conducted emissions, power converters, DC-bus.**

I. Introduction

With the advent and diffusion of power electronic circuits, electrolytic capacitors have become the preferable choice for making the DC buses of converters of all types [1], [2]. Compared to ceramic and polymer capacitors, they offer a high volumetric efficiency and price performance ratio [3]. Like any electrical component, the behavior of electrolytic capacitors is not ideal and depends on the type of voltage and current waveforms applied. In general, it is possible to assume that at very low frequencies an electrolytic capacitor exhibits an ideal behaviour, while at higher frequencies it is necessary to consider ohmic-inductive effects which alter its behaviour [4], [5]. Although this type of polarized capacitor is used for DC applications, in power electronic circuits the applied voltages and currents have higher frequency components due to the nonlinear behaviour of the switches [6]–[8]. The banks of electrolytic capacitors that constitute the DC bus of power converters are also in charge of suppressing the generated electromagnetic interference (EMI) and thus they have to be properly chosen to achieve the required filtering action [2], [9]. For a consistent design, proper frequency-dependent models are essential to describe the real behaviour of these components.

In order to represent the frequency behaviour of electrolytic capacitors over a wide frequency range, different models can be chosen, whose parameters are typically determined with tools such as vector network analyzers (VNAs) or impedance measurement bridges. These tools are typically expensive, especially because a wide frequency bandwidth is required for these types of applications. Moreover, electrolytic capacitors need to be polarized and therefore a DC voltage component must be applied during the measurement. This is possible in modern instruments, although typically voltage values are limited to some volts in practice. It is important to note that a bias voltage dramatically affects the parasitic resistance, as described in [10], as well as the current ripple [11]. Different alternative methods are described in literature [3]–[5], [10]–[12], even based on the analysis of the transient behavior of electrolytic capacitors. The majority of these paper discuss the role and the estimation of the parasitic resistance (ESR), while the equivalent series inductance (ESL) is not addressed. In [11] a simple method for the measurement of the ESL and ESR of electrolytic capacitors is presented. The parameters are determined, under some simplifying assumption, by measuring the step response of the capacitor. The step response is obtained by combining synchronous switches with a DC voltage source. The determination of the ESL is done analytically by estimating the initial slope of the response curve to an ideal step input. However, the nonideality of the step input (i.e., its non null rise time) may affect the correct determination of the ESL.

The aim of this work is to establish a simple and general method to estimate the parasitic parameters of electrolytic capacitors under any operating condition. Exploiting the energy conservation principle, it is demonstrated how it is possible to characterize an electrolytic capacitor by means of voltage and current measurements only. It is therefore possible to excite the capacitor under test with the desired waveform and to use an oscilloscope to acquire the signals. The required instruments are thus generally much cheaper than the VNAs that can be used for this type of application.

II. High-frequency equivalent circuit model of electrolytic capacitors

Polarized aluminum electrolytic capacitors comprise two electrically conductive layers that are separated by a dielectric

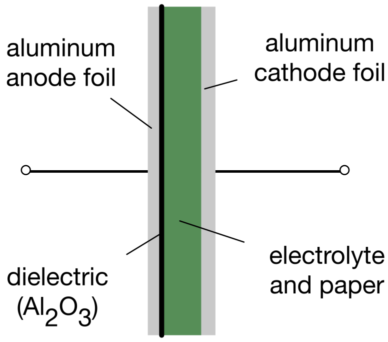

Fig. 1: Basic structure of an aluminum electrolytic capacitor.

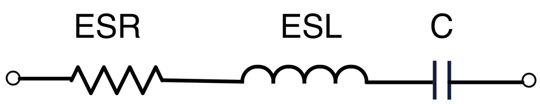

Fig. 2: Equivalent circuit for an electrolytic capacitor.

layer. One electrode (the anode) is made of an aluminum foil, a thin insulating layer of aluminum oxide built on the anode that is used as the dielectric, a liquid electrolyte (stored in the pores of an absorbent paper) that acts as the counter electrode, and a second aluminum foil (the cathode) that serves as a contact area for the current through the electrolyte. A basic structure of an aluminum electrolytic capacitor is depicted in Fig. 1. Usually the aluminum foils are electrochemically etched in order to increase the effective surface area and to obtain larger capacitance values. In this way, by the use of etching the dimension of electrolytic capacitor may be very compact. The behaviour of electrolytic capacitors over an extended frequency range can be described with equivalent circuits which result from the combination of passive components (resistors, inductors and capacitors) whose parameters are time independent in the frequency range of interest. The passive components used are introduced to represent the parasitic phenomena occurring in the component that become more and more evident as the frequency increases. In particular, the resistors are introduced to take into account the resistance of the component (due to wires, conductive foils, nonideality of the dielectric and soldering); the inductors take into account the inductive effects occurring in the component (due to the inductance of wires and to the wounded structure of the capacitor). In its most simplified (and implemented) version, the model for electrolytic capacitors consists of only three passive components connected in series: a resistor, an inductor and a capacitor. The model is depicted in Fig. 2, where ESR (equivalent series resistance) represents the overall effect of resistance of the component, ESL (equivalent series inductance) represents the overall effect of the inductance of the component, and C is the capacitance of the component. The impedance of this equivalent circuit is then used to represent the frequency behaviour of the component over an extended frequency range:

$$Z_C = ESR + j\omega ESL + \frac{1}{j\omega C}. \tag{1}$$

A procedure for the determination of the three parameters ESR, ESL and C is illustrated in the next sections.

III. Energy-based approach for the determination of the equivalent circuit parameters

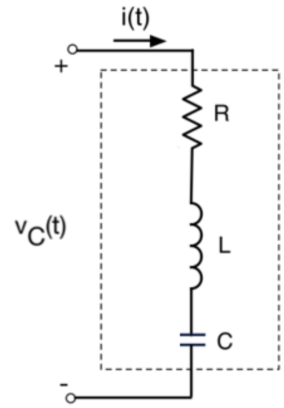

Fig. 3: Circuit for evaluating the energy of a real capacitor.

The basic idea behind the proposed method consists in determining the values of the parameters of the adopted circuit model (in this case a series R-L-C equivalent circuit) enforcing that the energy conservation principle for the component under test is fulfilled. In fact, for each instant of time, it must be true that the total energy $W_T(t)$ supplied to the capacitor corresponds to the sum of the energy $W_L(t)$ and $W_C(t)$ stored in the inductance L and capacitance C of the model, respectively, and the total energy $W_R(t)$ dissipated by the resistance R. Mathematically, it is:

$$W_T(t) = W_R(t) + W_L(t) + W_C(t). \tag{2}$$

where the total energy $W_T(t)$ is defined as:

$$W_T(t) = \int_{-\infty}^{t} v_C(\tau) i(\tau) d\tau, \tag{3}$$

where $v(t)$ and $i(t)$ are the electrolytic capacitor voltage and current, respectively. As it is possible to see in Fig. 3, the three parameters representing the real capacitor are crossed by the same current $i(t)$ and thus the energy contributions can be written as:

$$W_R(t) = R \int_{-\infty}^{t} i^2(\tau) d\tau \tag{4}$$

$$W_L(t) = \frac{1}{2} L i^2(t) \tag{5}$$

$$W_C(t) = \frac{1}{2C} \left(\int_{-\infty}^{t} i(\tau) d\tau \right)^2. \tag{6}$$

Considering n time instants, a system of n equations of the type of (2) can be set:

$$\begin{aligned} W_T(t_1) &= R\int_{-\infty}^{t_1} i^2(\tau)d\tau + \frac{1}{2}Li^2(t_1) + \frac{1}{2C}\left(\int_{-\infty}^{t_1} i(\tau)d\tau\right)^2 \\ W_T(t_2) &= R\int_{-\infty}^{t_2} i^2(\tau)d\tau + \frac{1}{2}Li^2(t_2) + \frac{1}{2C}\left(\int_{-\infty}^{t_2} i(\tau)d\tau\right)^2 \\ &\vdots \\ W_T(t_n) &= R\int_{-\infty}^{t_n} i^2(\tau)d\tau + \frac{1}{2}Li^2(t_n) + \frac{1}{2C}\left(\int_{-\infty}^{t_n} i(\tau)d\tau\right)^2. \end{aligned} \tag{7}$$

This system of equations can be used to derive the R-L-C parameters of the real equivalent circuit. Indeed, by measuring the electrolytic capacitor voltage and current it is then possible to calculate the energy at any time instant as well as the current integrals, and the only unknowns are the parameters R, L and C. In matrix form (7) becomes:

$$\mathbf{W} = \mathbf{M}\mathbf{X} \tag{8}$$

where $\mathbf{X}^T = [R \quad L \quad 1/C]$ is the parameter vector, $\mathbf{W}^T = [W_T(t_1) \ldots W_T(t_n)]$ is the vector containing the values of the energy calculated in the chosen time instants and

$$\mathbf{M} = \begin{bmatrix} \int_{-\infty}^{t_1} i^2(\tau)d\tau & \frac{i^2(t_1)}{2} & \frac{1}{2}\left(\int_{-\infty}^{t_1} i(\tau)d\tau\right)^2 \\ \vdots & \vdots & \vdots \\ \vdots & \vdots & \vdots \\ \int_{-\infty}^{t_n} i^2(\tau)d\tau & \frac{i^2(t_n)}{2} & \frac{1}{2}\left(\int_{-\infty}^{t_n} i(\tau)d\tau\right)^2 \end{bmatrix} \tag{9}$$

the coefficient matrix. In theory, being the system characterised by three unknowns only (R, L, C), three equations would guarantee an exact solution. However, in practice, the choice of the time instants dramatically affects the solution, with the risk of obtaining results that depend on the choice of the time instants. Since the energy of the system is described by the voltage and current functions over time calculated in only three points, it is possible that there are several sets of parameters that verify the system. In other words, different parameters could give rise to transients which, although different, are energetically equivalent in the chosen instants of time. The most intuitive solution consists in extending the system by introducing new equations for different instants of time and, in particular, distributed for the entire duration of the transient. In this way, we intend to impose that the solution of the system verifies the energy balance for the entire duration of the transient, thus reducing the possibility of finding incorrect values of the parameters. In this case, the system has more equations than unknowns and, therefore, it is not possible to obtain an exact solution. It is therefore necessary to solve the system by estimating the values of the parameters with numerical or statistical techniques. Several different tools can be chosen, ranging from traditional regression methods [13] to more recent optimisation or artificial intelligence algorithms [14]. Being the system not particularly complicated, the generalized least-square method is used.

IV. Experimental Setup

In order to evaluate $\mathbf{W}$ and $\mathbf{M}$ at the generic instant of time t_i, the capacitor voltage $v(t)$ and current $i(t)$ should be known from $-\infty$ to t_i (see (3) and (9)), making the calculation difficult (if not impossible). A simplification consists in assuming a circuit configuration where $v(t) = 0$ and $i(t) = 0$ from $-\infty$ to an instant of time t_0, when a constant voltage is applied to the real capacitor. In this way, the integrals in $\mathbf{W}$ and $\mathbf{M}$ reduce to integrals from t_0 to t. Experimentally, the circuit depicted in Fig. 4 can be used, where the resistor R_{aux} has the purpose to increase the time constant of the circuit (and, in turn, the transient duration) and allow the current to be measured. The constant voltage is applied as a square waveform by means of a signal generator. This requires the very first transient to be triggered in order to ensure that there is not any residual charge in the capacitor (and thus $v(t) = 0$ and $i(t) = 0$). Alternatively, a simpler way to proceed consists in setting the square waveform frequency low enough to have a corresponding period longer than the transient duration (viz., several times the time constant of the circuit). In this way, any circuit transient can be triggered in order to perform the analysis. In this paper a square waveform with 5 Hz frequency was chosen, in order to have a period of 200 ms which, for a resistance $R_{aux} = 5\Omega$, is enough to test capacitors of capacitance up to 1 mF. The square waveform was generated with a signal generator (10 μHz - 50MHz) and the signals were acquired with an R&S RTO 1004 oscilloscope with a bandwidth of 600 MHz. To increase the voltage applied to the capacitor and provide the required power a 10 W Philips PM 5175 power amplifier with a DC-1 MHz bandwidth is also used. The amplifier gain is set to 14 dB. The effective square voltage $v_g(t)$ applied to the series of R_{aux} and the capacitor under test presents a 70 ns rise edge, due to the presence of the amplifier. Nevertheless, the setup presents a frequency bandwidth wide enough for testing electrolytic capacitors with resonance frequency in the order of hundredth kHz.

A. Results

The proposed method has been tested for characterising an electrolytic capacitor with a rated capacitance of 470μF. The voltage signals (across the output and the auxiliary resistor) have been acquired for 20ms, that is the expected transient duration based on the rated capacitance and auxiliary resistance R_{aux} values. The resulting waveforms are shown in Fig. 5a for the entire transient, with a zoomed view of the first transient time instants in Fig. 5b. As discussed in Sec. III, the choice of the time instants in which the energy $\mathbf{W}$ and the coefficients $\mathbf{M}$ are calculated can have a significant impact on the system solution. In particular, the resistance R and inductance L are parasitic elements (they are respectively the ESR and ESL) and therefore their energy contributions are expected to be much smaller than that of the capacitance C. Furthermore, the effect of the inductance is reasonably visible in the initial instants of the transient, in which the current variation is very rapid. With reference to the voltage and current of the capacitor, two transients can be identified:

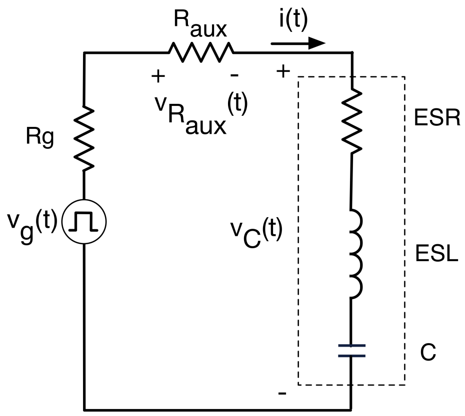

Fig. 4: Equivalent circuit of the experimental setup for the determination of parasitic parameters of an electrolytic capacitor.

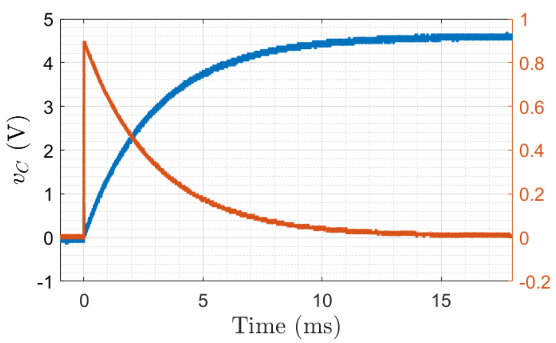

(a)

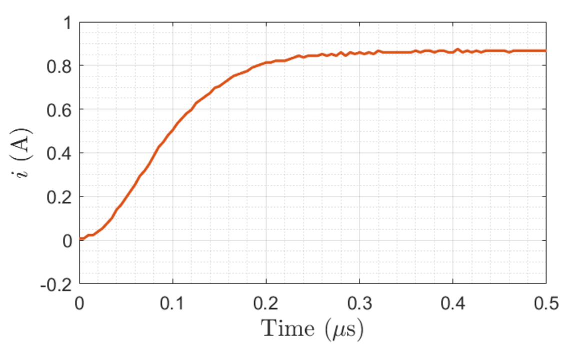

(b)

Fig. 5: Transient waveforms of (a) the voltage and current across the capacitor for the entire transient and (b) the capacitor current for the first time instants.

- a fast transient dominated by R and L, where the current that crosses R_{aux} and, in turn, the capacitor is rapidly increasing (see Fig. 5b);
- a slower transient dominated by R and C (see Fig. 5a).

As a first approximation, in the slow transient, it may be reasonable to neglect also the contribution of R, but not much is saved in computational terms. Therefore, its contribution is

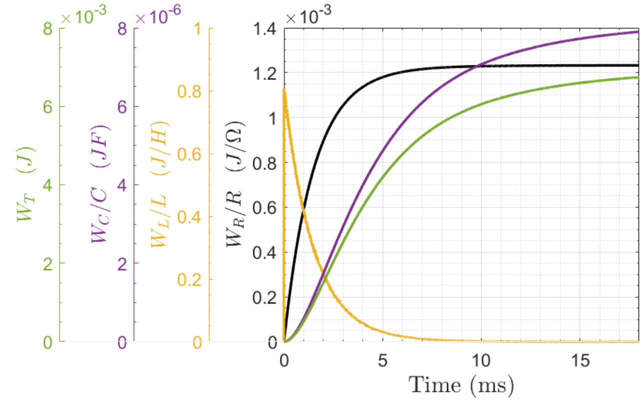

(a)

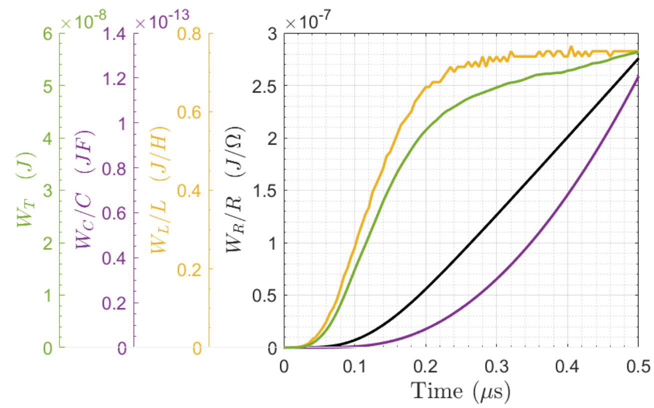

(b)

Fig. 6: Transient behaviour of the capacitor energy $W_T(t)$ and the matrix coefficients described in (9) for (a) the entire transient and (b) for the first time instants.

always considered, ensuring greater accuracy of the solution.

Due to the numerical nature of the system solution, it is necessary to consider the values of the coefficients for the chosen n time instants. The values of the energy and the coefficients calculated in time instants of the slow transient are much larger with respect to the ones of the fast transient with the risk of leading to a bad-conditioned problem and thus compromising the system solution. This can be appreciated from the plots of Figs. 6a and 6b, that show the behaviour of the capacitor energy $W_T(t)$ and the matrix coefficients for the entire transient and the first instants, respectively. It can be noticed that the same quantities can have very different values depending on the time instant in which they are calculated, as expected. To preserve the conditioning of the problem, a restricted number of time instants should be chosen. Moreover, for null values of $i(t)$ (found in the slow transient), Fig. 6a clearly shows that W_C intrinsically dominates over W_L and W_R and thus the capacitance C can be assumed nearly uniquely determined (as already mentioned no contributions are neglected *a priori*). The second consideration focuses on the fast transient. Indeed, in this case, the combination of R, L

TABLE I: Parameter values of two capacitors of the same brand with rated capacitance $C_{rated} = 470\mu$F and 35 V voltage.

First Capacitor			
	R [mΩ]	L [nH]	C [μF]
Proposed method	69.05	114.3	596.4
VNA 1	93	72.5	580.2
VNA 2	–	70	–
Second Capacitor			
	R [mΩ]	L [nH]	C [μF]
Proposed method	19.48	92.88	572.7
VNA 1	100	58.3	560.62
VNA 2	–	47	–

and C considerably contributes to the shape of $i(t)$, meaning that different sets of values can verify the energy balance. Thus the number of time instants (and thus the equations) should be increased to capture the features of the effective $i(t)$ curve. Heuristically, it is reasonable to choose 4 or 5 points for both the rising edge and the maxima values. Overall, after several attempts, $n = 11$ has been considered sufficient to achieve a stable and repeatable solution. In particular, 10 points equally distributed in the fast transient (namely comprised between $t = 0$ and $t = 0.4\mu$s) and one at the end of the transient (at $t =$ 19ms to properly estimate C). The resulting values of the R, L and C parameters are shown in Tab. I and compared with the values estimated with two VNAs, the former (VNA 1) with a bandwidth of 5 Hz – 3 GHz and the possibility to apply a DC-bias and the latter (VNA 2) with a bandwidth of 300 kHz – 3.6 GHz. The DC-bias of VNA 1 was however limited to a few volts (3 V) only in order to avoid overload of the VNA input.

The measurement with both the proposed method and the VNA 1 shows that the capacitance values of both the electrolytic capacitors are larger than the rated one; nothwithstanding, the measured values are within the 20% tolerance of the component capacitance. It was not possible to estimate the capacitance with VNA 2 as the lowest frequency of the VNA (300 kHz) is beyond the resonance frequency of the capacitor. As regards the parasitics of the capacitors, the comparison of results shows that for both capacitors the inductance estimated with the proposed method is higher than that measured with both VNAs. In any case, the difference between the inductance values of the two capacitors estimated with the proposed method is analogous to what measured with the two VNAs. This can be attributed to some parasitic inductance in the experimental setup used in the proposed method (connections, auxiliary resistor, etc.), which needs to be optimized. As regards the parasitic resistance, it can be seen that the values measured with the VNA 1 are larger than those obtained with the proposed method. Furthermore, the VNA 1 gives about the same parasitic resistance for both the tested capacitors, whereas the proposed method shows a difference of about 50 mΩ in the two cases (the component with largest capacitance and inductance has also the largest resistance). The larger resistance found in the VNA measurement may be due to the connector on which the component was mounted and the calibration procedure, that needs to be improved. As for the capacitance, it was not possible to estimate the parasitic resistance with VNA 2 since its minimum frequency is beyond the resonance frequency of the electrolytic capacitor.

Overall, it is important to notice that in order to estimate the R and C parameters the starting operating frequency of a VNA should be the lowest possible, whereas in order to estimate L the maximum frequency should be beyond the resonance frequency of the electrolytic capacitor. These wideband instruments may be very expensive and alternative methods for the characterisation of electrolytic capacitors are then useful. Moreover, the proposed energy-based method allows the capacitor parameters to be estimated at any operating conditions provided that its voltage and current can be acquired. When testing electrolytic capacitors, which are polarized during their operation, the applied DC voltage component plays a crucial role and the possibility of applying any voltage level allows a complete characterization of the components where required.

V. CONCLUSION

The proposed method has been established to determine the parasitic resistance ESR and inductance ESL of electrolytic capacitors according to a series R-L-C model. Enforcing the conservation of energy for different time instants of the transient, it is possible to define a system of equations where the R, L and C parameters are the only unknowns. Despite just three equations would be enough to determine a solution of the system, the arbitrary choice of the time instants in which the energy is calculated may affect the final results. To overcome this issue, more equations have been added to the set to ensure the energy balance is verified for the entire duration of the transient. However, being the number of equations higher that the number of unknowns (the R-L-C parameters), the system was solved numerically with a least-square algorithm. The research revealed that a limited number of time instants (and in turns of equations) is required to have a stable and repeatable solution, i.e., independent of the selected time instants. In particular, it was found that about ten points are necessary to describe the first part of the transient whereas at least one point is required when the transient is almost over. The R-L-C parameters of two capacitors of the same brand with the same rated capacitance and voltage have been estimated. The comparison with measurements carried out with two different VNAs shows a good agreement. The method has been proven to be effective to characterise electrolytic capacitors, offering the possibility to test them in any operating condition, and can therefore considered a valid alternative to expensive instruments such as wideband VNAs.

REFERENCES

[1] B. P. McGrath and D. G. Holmes, "A general analytical method for calculating inverter dc-link current harmonics," *IEEE Transactions on Industry Applications*, vol. 45, no. 5, pp. 1851–1859, Jul. 2009.

[2] M. Vujacic, M. Hammami, M. Srndovic, and G. Grandi, "Theoretical and experimental investigation of switching ripple in the dc-link voltage of single-phase h-bridge pwm inverters," *Energies*, vol. 10, no. 8, Aug. 2017.

[3] A. M. R. Amaral and A. J. M. Cardoso, "An experimental technique for estimating the esr and reactance intrinsic values of aluminum electrolytic capacitors," in *2006 IEEE Instrumentation and Measurement Technology Conference Proceedings*, Sorrento, Italy, 24-27 Apr. 2006, pp. 1820–1825.

[4] Y.-M. Chen, M.-W. Chou, and H.-C. Wu, "Electrolytic capacitor failure prediction of lc filter for switching-mode power converters," in *Fourtieth IAS Annual Meeting. Conference Record of the 2005 Industry Applications Conference, 2005.*, vol. 2, Hong Kong, China, 2-6 Oct. 2005, pp. 1464–1469 Vol. 2.

[5] K. Harada, A. Katsuki, and M. Fujiwara, "Use of esr for deterioration diagnosis of electrolytic capacitor," *IEEE Transactions on Power Electronics*, vol. 8, no. 4, pp. 355–361, Oct. 1993.

[6] A. Mariscotti, L. Sandrolini, and M. Simonazzi, "Supraharmonic emissions from dc grid connected wireless power transfer converters," *Energies*, vol. 15, no. 14, Jun. 2022. [Online]. Available: https://www.mdpi.com/1996-1073/15/14/5229

[7] M. Simonazzi, L. Sandrolini, M. Iotti, and A. Mariscotti, "Deep-learning based transient identification in switched-mode power supplies conducted emissions," in *2022 International Symposium on Electromagnetic Compatibility – EMC Europe*, Gothenburg, Sweden, 5-8 Sep. 2022, pp. 410–414.

[8] M. Simonazzi and L. Sandrolini, "Conducted emission analysis of a near-field wireless power transfer system," in *2021 IEEE 15th International Conference on Compatibility, Power Electronics and Power Engineering (CPE-POWERENG)*, Florence, Italy, 14-16 Jul. 2021, pp. 1–6.

[9] B. Kerrouche, M. Bensetti, and A. Zaoui, "New emi model with the same input impedances as converter," *IEEE Transactions on Electromagnetic Compatibility*, vol. 61, no. 4, pp. 1072–1081, Jul. 2019.

[10] P. Venet, F. Perisse, M. El-Husseini, and G. Rojat, "Realization of a smart electrolytic capacitor circuit," *IEEE Industry Applications Magazine*, vol. 8, no. 1, pp. 16–20, Aug. 2002.

[11] K. Tsang and W. Chan, "Simple method for measuring the equivalent series inductance and resistance of electrolytic capacitors," *IET Power Electronics*, vol. 3, no. 4, pp. 465–471, July 2010.

[12] M. Gasperi, "A method for predicting the expected life of bus capacitors," in *IAS '97. Conference Record of the 1997 IEEE Industry Applications Conference Thirty-Second IAS Annual Meeting*, vol. 2, New Orleans, LA, USA, 5-9 Oct. 1997, pp. 1042–1047 vol.2.

[13] R. A. Berk, *Regression Analysis: A Constructive Critique*, 1st ed. SAGE Publications, Inc., 2004.

[14] D. E. Rumelhart, G. E. Hinton, and R. J. Williams, *Learning Internal Representations by Error Propagation*. Cambridge, MA, USA: MIT Press, 1986, p. 318–362.